



Contents lists available at SciVerse ScienceDirect

Solid State Sciences

journal homepage: [www.elsevier.com/locate/ssscie](http://www.elsevier.com/locate/ssscie)

# The route to highly stable $\text{MeB}_x\text{N}_y\text{C}_z$ molecular wheels. I. The features of preliminary results

I. Boustani<sup>a,\*</sup>, R. Pandey<sup>b</sup><sup>a</sup>Bergische Universität Wuppertal, FB C - Mathematik und Naturwissenschaften, Gaußstraße 20, 42119 Wuppertal, Germany<sup>b</sup>Michigan Technological University, Department of Physics, Houghton, MI 49931, USA

## ARTICLE INFO

## Article history:

Received 24 October 2011

Received in revised form

9 March 2012

Accepted 14 March 2012

Available online xxx

## Keywords:

Molecular wheels

Titanium boride clusters

Boron wheels

## ABSTRACT

By means of *ab initio* quantum chemical methods we have determined the energies and electronic structures of molecular wheels  $\text{TiB}_n$ ,  $\text{TiB}_n\text{N}_{10-n}$ ,  $\text{TiC}_n\text{N}_{10-n}$  and  $\text{TiC}_n\text{B}_{10-n}$  (for  $n = 0-10$ ). The ground state energies and the corresponding spin states of each atom, cluster and molecular wheel were calculated first in the framework of Hartree-Fock self-consistent-field (HF-SCF) using minimal and more accurate basis sets STO-3G and 6-31G. Computations at higher level and accuracy are processing in a follow-up study. The most stable wheel system is  $\text{TiC}_n\text{B}_{10-n}$  (for  $n = 5-10$ ). Thereof particularly highly stable is the  $\text{TiC}_5\text{B}_5$  molecular wheel followed by the  $\text{TiC}_6\text{B}_4$ . At the HF-SCF/6-31G level, however, we have calculated the wheel system  $\text{MeC}_5\text{B}_5$  considering for Me, the first row of transition metal atoms  $\text{Me} = \text{Sc}, \text{Ti}, \text{V}, \text{Cr}, \text{Mn}, \text{Fe}, \text{Co}, \text{Ni}, \text{Cu}, \text{and Zn}$ . The molecular wheel  $\text{MeC}_5\text{B}_5$  favours Sc atom at the centre, but also Ti and Fe are the next favoured atoms.

© 2012 Elsevier Masson SAS. All rights reserved.

## 1. Introduction

Interest in synthesis and exploration of structure and energetics of boron clusters and boron-compounds has both academic and practical aspects. Such structures should have a wide variety of applications. The reason lies simply by the atomic boron which is the only element except carbon that can build molecules of any size by covalently bonding to itself. Due to  $sp^2$  hybridization of the valence electrons, large coordination number and short covalent radius, boron prefers to form strong directional bonds with various elements. Due to its electron deficiency boron makes multi-centre bonds where pair of electrons is shared between two atoms and more [1].

At the molecular level, elemental boron clusters  $\text{B}_n$  for ( $n = 2-8$ ) were investigated in 1990 by I. Boustani et al. (unpublished results) using a double- $\zeta$  basis set with polarization function (DZ + P) in the framework of the Hartree-Fock (HF) self-consistent-field (SCF) theory and configuration interaction (CI), published in part 1991 [2]. The most interesting structure is the so-called molecular wheel  $\text{B}_8$ , which is composed of a central boron atom surrounded by a regular boron heptagon. The ground state of  $\text{B}_8$  molecular wheel is  $D_{7h}$  ( $^3A_2$ ). The bondlength of the heptagon is 1.516 Å, and the distance to the central atom is about 1.747 Å. Further pure boron

clusters have been extensively explored namely both theoretically [3] and experimentally [4]. Thus boron clusters  $\text{B}_n$  were found to exhibit planar configurations for  $n \leq 14$  and consequently are aromatic. The aromatic (planar) boron clusters possess more circular shapes whereas anti-aromatic ones are elongated. Recent experimental [5] and theoretical [6] studies on boron clusters show that the anionic and neutral  $\text{B}_{19}$  clusters are the largest two-dimensional aggregates of boron.

On the other hand, small clusters of the neighbouring element carbon  $\text{C}_n$ , determined for  $\leq 10$ , are linear chains for odd  $n$  and closed rings for even  $n$  [7]. Carbon clusters  $\text{C}_n$  for ( $6 \leq n \leq 13$ ) were also investigated Slanina et al. [8]. They found that the carbon clusters  $\text{C}_n$  for  $\leq 10$  have also linear chains for odd  $n$  and cyclic structures for even  $n$ . But however, the carbon clusters  $\text{C}_{11}$ ,  $\text{C}_{12}$  and  $\text{C}_{13}$  have cyclic structures. Larger carbon clusters  $\text{C}_n$  for ( $14 \leq n \leq 24$ ,  $n$  even) were investigated by Jones and Seifert [9]. They found that the carbon clusters have chains, rings, graphitic plate, bowl and cage-like structures. They also found that the most stable isomers for the carbon clusters  $\text{C}_{14}$ ,  $\text{C}_{16}$  and  $\text{C}_{18}$  have monocyclic ring structures.

Binary compounds of boron and carbon atoms, known as boron carbides, are the most widely investigated compounds. The rhombohedral elemental cell of a single-crystal boron carbide is composed of boron icosahedra residing at each vertex containing three atomic linear chains, like C–B–C or C–C–C, located at the main cell diagonal of the rhombohedron [10]. However, small neutral and charged boron carbide  $\text{B}_{8-m}\text{C}_m$  clusters for  $m = 1$  to 3

\* Corresponding author. Tel.: +49 202596665.

E-mail addresses: [boustani@t-online.de](mailto:boustani@t-online.de), [boustani@uni-wuppertal.de](mailto:boustani@uni-wuppertal.de) (I. Boustani).

are recently studied by S. S. Park [11] using density functional theory. He investigated eight  $B_7C^{-1}$ , twelve  $B_6C_2$ , and twelve  $B_5C_3^{+1}$  isomers and found that the most stable structures are molecular wheels with a central boron atom. Molecular-dynamics simulation of structural and thermodynamic properties of cubic boron nitride c-BN were studied by Sekkal et al. [12] using well-tested Tersoff potential. They predicted the corresponding various physical quantities including the thermal expansion coefficient and heat capacity. They extended these simulations to study liquid boron nitride at various densities.

Titanium carbide clusters were also studied by Wang et al. [13]. They reported the vibrationally resolved photoelectron spectra of a series of  $TiC_x^{-1}$  clusters for  $x = 2-5$  and observed that ground state vibrational frequencies and electron affinities are tentatively interpreted to support ring-type structures for these clusters. Furthermore, small clusters of metal boride  $MeB_n$  ( $n \leq 7$ ) particularly those of transition metals (Cr to Ni) were investigated by X. Liu et al. [14]. They used first-principles DFT-GGA methods and studied their electronic and magnetic properties. They found that  $MeB_n$  clusters with  $n \leq 5$  have planar triangular geometries, those with  $n = 6$  have wheel forms, while  $MeB_n$  clusters with  $n = 7$  are three-dimensional. Metal-boron molecular wheels were studied by Pu et al. [15] using also density functional theory. They found that  $B_9$  and  $B_{10}$  rings accommodate the first row of transition metals. Microstructure and properties of superhard Ti–B–C–N films deposited on stainless steel substrated by a dc unbalanced magnetron sputtering were studied by I.-W. Park et al. [16]. They found that the hardness of the Ti–B–C–N films increases with the increase of N content up to a maximum value of approximately 45 GPa at 10 at. % N, with a subsequent decrease in hardness at higher N.

The purpose of this study is to show first that the formation of  $TiB_n$  systems, composed of a single transition metal atom like Ti and of boron atoms embedded one by one, favours aromatic two-dimensional (2D) over three-dimensional (3D) structures, as it is the case of planar boron clusters, and leads to molecular wheels. Furthermore it is to show the route of stability of the molecular wheels when boron atoms are replaced by nitrogen then by carbon atoms. Since the metal atom Ti can link and accommodate in a plane maximum 10 boron atoms so that the surrounding binding boron atoms around the central metal atom just building reasonable bonds to each other and also to the centre Ti. Therefore the size of the molecular wheels beside Ti atom is limited by 10 atoms and thus the stability of the  $MeB_xN_yC_z$  wheels does not depend more on the size but only on the combination of boron, nitrogen and carbon atoms around the central transition metal atoms. Thereupon, we will study the geometry, electronic structures and cluster stability of the molecular wheels of the  $TiB_n$ ,  $TiB_nN_{10-n}$ ,  $TiC_nN_{10-n}$  and  $TiC_nB_{10-n}$  (for  $n = 1-10$ ) systems as well as  $MeC_5B_5$ , for (Me = Sc, V, Cr, Mn, Fe, Co, Ni, Cu, Zn). The paper is organized as follows: the computational methods will be described then discussion and results and finally summary and conclusions.

## 2. Computational details

*Ab initio* quantum chemical methods for solving the many-electron problems in the framework of the Hartree-Fock self-consistent-field (HF-SCF) were applied to determine the ground state energies of the molecular systems. All-electron calculations in the current work were performed using STO-3G and 6-31G basis sets. Computations at higher level of theory with more accurate and extensive functionals, pseudopotentials and basis sets are in process in a follow-up study [17]. The optimization procedure, based on the analytical gradient method, has been carried out for the ground state energies using the restricted and unrestricted

Hartree-Fock theory for closed- and open-shell systems, using the minimal basis set STO-3G. The most stable molecular wheel  $MeC_5B_5$  was calculated for the first row of metal atoms at the HF-SCF/6-31G level of theory. In order to determine the stability of the cluster compounds we have calculated the binding energy ( $E_b$ ) in eV/atom as follows:

$$E_b = \frac{1}{n} \{ E(\text{Me}) + xE(\text{B}) + yE(\text{C}) + zE(\text{N}) - E(\text{MeB}_x\text{C}_y\text{N}_z) \} \quad (1)$$

where  $n$  is the total number of atoms in the clusters,  $E(\text{Me})$  is the energy of atomic transition metal Me = Sc, Ti, V, Cr, Mn, Fe, Co, Ni, Cu and Zn, where  $E(\text{B})$ ,  $E(\text{C})$ , and  $E(\text{N})$  are the energies of boron, carbon, and nitrogen atoms, respectively.  $E(\text{MeB}_x\text{C}_y\text{N}_z)$  is the energy of the cluster or of the molecular wheel, while  $x$ ,  $y$  and  $z$  are the number of compounds in the cluster or wheel. In all calculations we have considered symmetry constraints in the form of a point group symmetry. We have also calculated different spin states for each atom and cluster selecting the corresponding lowest energy to be the ground state energy. These calculations were carried out using the Gaussian 03 [18] and Gamess\_UK [19] program packages.

Concerning the calculations at the HF-SCF level of theory and at the basis set STO-3G, we are aware of the limitation of this method as well as the basis set to get a qualitative guidance about the stability of the systems, when adding boron atoms one by one around Ti to obtain the molecular wheel, then replacing boron by nitrogen or carbon atoms to achieve larger stability. However and as mentioned above, we are working in a follow-up paper [17] in which qualitative and quantitative calculations at higher quality basis sets and pseudopotentials as well as much more accurate functionals beyond the HF-SCF to verify and confirm the trend in stability of the system predicted at the HF-SCF/STO-3G level of theory.

## 3. Results and discussion

Earlier *ab initio* calculations of boron clusters have shown that small clusters favour 2D quasiplanar formations [20,21]. But how do behave these structures as soon as we dope a single transition metal atom into the cluster? The best way to approach the answer is to take a metal atom like Ti adding boron atoms solong until acheiving stable structures. The first route is the planar system  $TiB_n$  (for  $n = 1-10$ ) starting by the  $TiB$  dimer adding atom by atom building a cyclic ring around Ti. In order to show that the  $TiB_n$  clusters favour 2D structures we have determined also some isomers of arbitrary 3D structures mostly pyramids with an apex or central Ti atom. These calculations were carried out at the HF-SCF/STO-3G level of theory considering doublet- and triplet-states for clusters with odd and even  $n$ , respectively.

### 3.1. The 2D $TiB_n$ systems

The linear  $TiB$  and the equilateral triangle  $TiB_2$  with Ti as an apex atom have been determined having binding energies of 1.83 and 2.32 eV/atom. The linear  $TiB$  molecule of  $C_{\infty v}(^2\Sigma_g^-)$  symmetry and state has a bondlength of 1.84 Å. Concerning  $TiB_2$ , the atomic distance between the apex atom Ti and both boron atoms in the triangular trimer is about 2.18 Å, while the bondlength between both boron atoms is about 1.64 Å. The 2D structure  $TiB_3$  cluster is a rectangle in which the Ti atom is connected to three bonding boron atoms forming an arc, as shown in Fig. 1. The calculated  $E_b$  of the planar  $TiB_3$  cluster of  $C_{2v}(^2B_2)$  symmetry and state is about 2.47 eV/atom. The bondlength between the Ti atom and the middle boron atom is 2.14 Å, while the it is about 2.08 Å to the outer atoms. The atomic distance between the boron atoms is 1.54 Å. The 2D

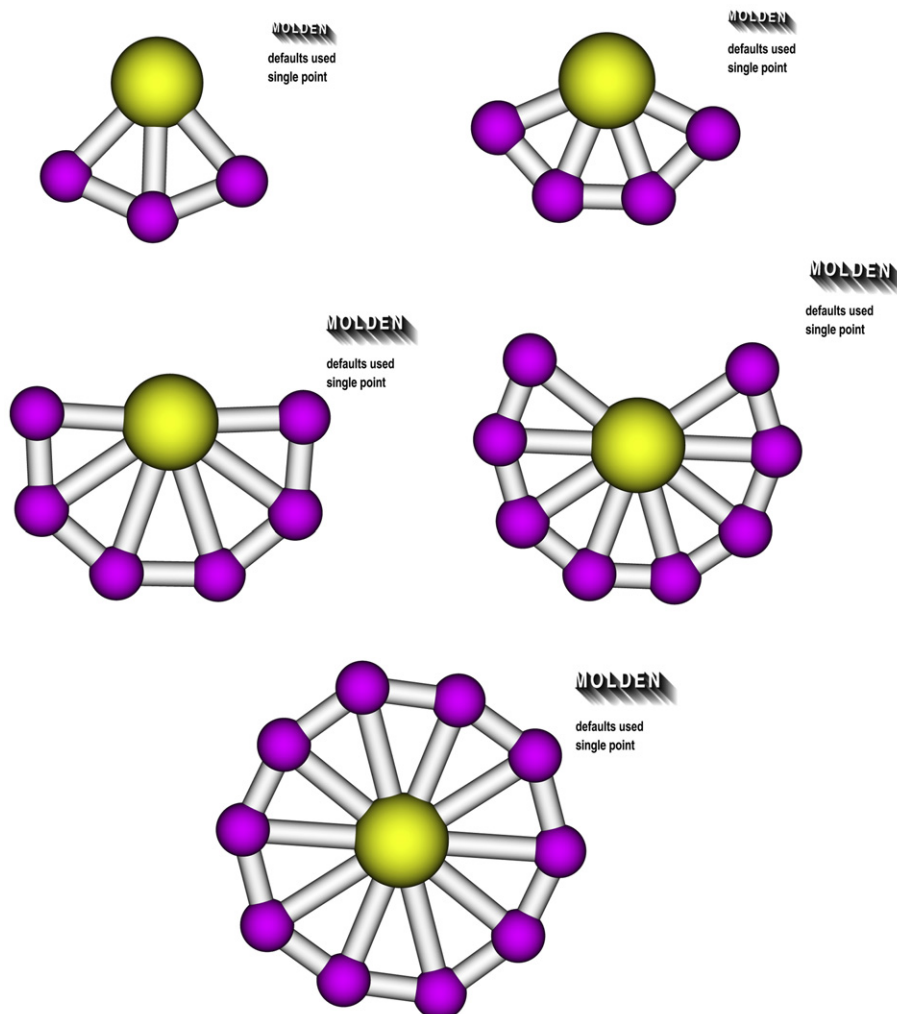


Fig. 1. 2D structures  $\text{TiB}_3$ ,  $\text{TiB}_4$ ,  $\text{TiB}_6$ ,  $\text{TiB}_8$  and  $\text{TiB}_{10}$ .

structure of the  $\text{TiB}_4$  cluster is developed from the planar  $\text{TiB}_3$  cluster, as shown in Fig. 1. The  $E_b$  of  $\text{TiB}_4$  determined in  $C_{2v}(^3A_1)$  symmetry and state is about 2.88 eV/atom. The distances in planar  $\text{TiB}_4$  between Ti atom and the arc of four boron atoms are 2.25 Å to the middle atoms, while 2.07 Å to the outer atoms. The atomic distance between the middle boron atoms is 1.50 Å, while the distance to the outer atoms is 1.53 Å. The planar structure of  $\text{TiB}_5$  of  $C_{2v}(^2B_2)$  symmetry and state with an  $E_b$  of 3.23 eV/atom is a further development of  $\text{TiB}_4$ . The average bond distance from Ti atom to the central arc of boron atoms is 2.15 Å, while the average bond length between the boron atoms is about 1.53 Å.

The same tendency of stability by the clusters with even  $n$  can be ascertained by the 2D clusters  $\text{TiB}_6$  and  $\text{TiB}_8$ , as shown in Fig. 1. The stability of clusters  $\text{TiB}_6$  of  $C_{2v}(^3A_1)$  and  $\text{TiB}_8$  of  $C_{2v}(^3B_2)$  symmetry and state is determined to 3.17 and 3.41 eV/atom, respectively. Regarding the planar  $\text{TiB}_6$  structure, the bond length between the Ti atom to the middle boron atoms of the arc is about 2.29 Å, while the distance to next two atoms is 2.27 Å, then to outer atom is 2.08 Å. The atomic distance between the middle boron atoms is about 1.48 Å, while it is 1.50 and 1.52 Å to the next and over next boron atoms. The average bond length between Ti atom in  $\text{TiB}_8$  and the eight boron atoms is about 2.08 Å, while the average atomic distance between the boron atoms is about 1.59 Å.

The stability of the planar  $\text{TiB}_7$  and  $\text{TiB}_9$  clusters of odd boron atoms, both of  $C_{2v}$  symmetry, obtained from planar  $\text{TiB}_6$  and  $\text{TiB}_8$  clusters by adding further boron atom to each one, is 3.27 and 3.42 eV/atom, respectively. The average atomic distance between Ti atom and the arc of boron atoms for  $\text{TiB}_7$  of  $C_{2v}(^2A_1)$  is about 2.20 Å and the average bond length between boron atoms is about 1.58 Å. The  $\text{TiB}_9$  cluster optimized in  $C_{2v}(^2B_2)$  symmetry and state approaches a wheel structure with an average radial distance of 2.22 Å, while the average distance between the peripheral boron atoms is about 1.52 Å. The final 2D structure  $\text{TiB}_{10}$  is a wheel with a  $D_{10h}$  symmetry calculated in  $D_{2h}(^3B_{3g})$  symmetry and state as shown in Fig. 1. The calculated  $E_b$  of the 2D  $\text{TiB}_{10}$  structure is about 3.69 eV/atom. The atomic distance between the Ti atom and the cyclic boron atoms is about 2.39 Å, while the bond length of the decagon is about 1.48 Å.

### 3.2. The 3D $\text{TiB}_n$ systems

The 3D structure of the  $\text{TiB}_3$  cluster is a trigonal pyramid of  $C_{3v}(^4A_1)$  symmetry and state in which Ti is the apex atom, is shown in Fig. 2. The calculated  $E_b$  of the trigonal pyramid  $\text{TiB}_3$  cluster is about 2.05 eV/atom. The distance between the triangle boron atoms and the apex Ti atom is about 1.85 Å, while the bond length of the triangle boron atoms is 1.56 Å. The binding energy of the

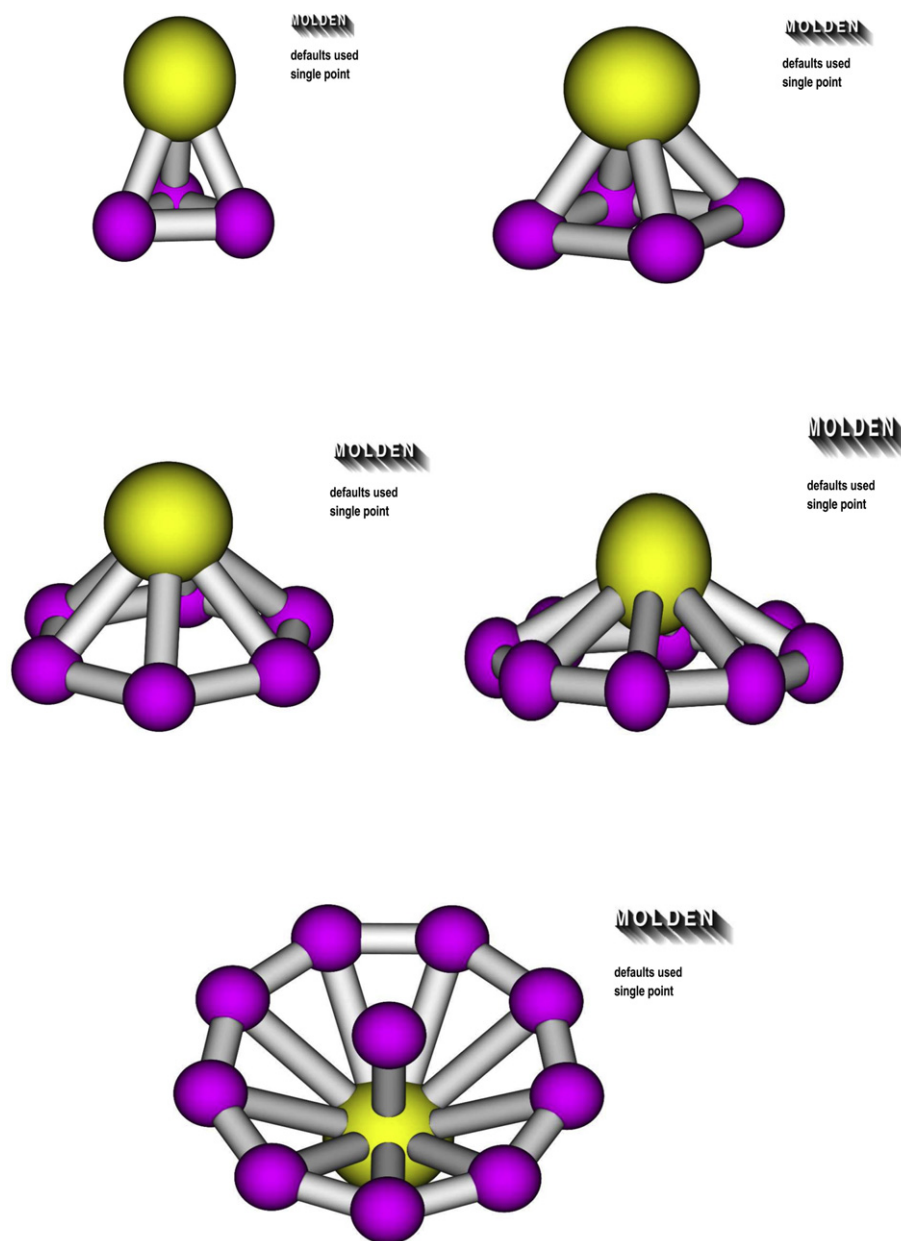


Fig. 2. 3D structures  $\text{TiB}_3$ ,  $\text{TiB}_4$ ,  $\text{TiB}_6$ ,  $\text{TiB}_8$  and  $\text{TiB}_{10}$ .

tetragonal pyramid  $\text{TiB}_4$  of  $C_{4v}(^3A_1)$  symmetry and state, as presented in Fig. 2, is about 2.42 eV/atom. The apex Ti atom departs to the boron square about 2.46 Å, while the bondlength of the square is about 1.56 Å. The  $E_b$  of the pentagonal pyramid  $\text{TiB}_5$  of  $C_{5v}(^2A_1)$  symmetry and state is about 3.11 eV/atom. The atomic distance between the apex Ti and the five fold boron atoms is 2.23 Å, while the bondlength of the pentagon is about 1.52 Å.

The 3D structures, the hexagonal pyramid  $\text{TiB}_6$  of  $C_{6v}(^3A_1)$  symmetry and state and the octagonal pyramid  $\text{TiB}_8$  with  $C_{8v}(^3B_1)$  symmetry and state, as presented in Fig. 2, are less stable than the 2D structures, where their binding energies are assigned to 3.07 and 3.30 eV/atom, respectively. For the  $\text{TiB}_6$  cluster, the atomic distance between the apex Ti and the hexagon is 2.29 Å, while the bondlength of the hexagon is about 1.53 Å. For the  $\text{TiB}_8$  cluster, the atomic distance between the apex Ti and the octagon is 1.94 Å, while the bondlength of the octagon is about 1.49 Å. The heptagonal pyramid  $\text{TiB}_7$  with an  $E_b$  of 3.25 eV/atom is slightly less stable

than the planar one. The atomic distance of the apex Ti atom to the heptagon is about 2.19 Å and the bondlength of the heptagon is about 1.51 Å.

The 3D  $\text{TiB}_9$  cluster of  $C_{8v}$  symmetry, calculated in  $C_{2v}(^2B_2)$  symmetry and state, is an octagonal umbrella or satellite dish in form of an octagon in which Ti atom is located at the centre and bonded to boron atom localized at the focus. The corresponding  $E_b$  is about 3.32 eV and thus less stable than the planar one. The atomic distance from the Ti atom to the octagon is 2.34 Å and to the boron atom at the focus is 2.01 Å, while the bondlength of the octagon is about 1.49 Å. Finally we determined the 3D structure of  $\text{TiB}_{10}$  cluster of  $C_{9v}$  symmetry, calculated in  $C_s(^3A'')$  symmetry and state. It is a nonagonal umbrella or satellite dish with Ti at the centre of the nonagon bonded to boron atom at the focus, as can be seen in Fig. 2. The calculated  $E_b$  is about 3.56 eV and thus is less stable than the planar one. The atomic distance between the Ti atom and the cyclic boron atoms is about 2.36 Å, and the distance to



the boron atom lying at the focus is 2.03 Å, while the bondlength of the nonagon is about 1.48 Å.

Due to the fact that the all 2D structures of  $TiB_n$  are energetically favoured over the 3D pyramids, we have considered the planar clusters and presented their stability in Fig. 3, as a function of cluster size or the number of boron atoms. It can be asserted that the function  $E_b$  of the system  $TiB_n$  for ( $n = 1-10$ ) increases with increasing the number of boron atoms, represented by the stars. In addition, we have selected some 2D and 3D structures of  $TiB_n$  for ( $n = 3, 4, 6, 8$  and 10) and presented in Figs. 1 and 2, respectively. In addition, we have listed the stability of the 2D and 3D structures and the corresponding point group symmetry and spin states in Table 1.

### 3.3. The $TiB_nN_{10-n}$ system

After obtaining the titanium boron molecular wheel, we have started to dope this wheel with nitrogen atoms by replacing boron by nitrogen atoms one by one calculating the  $E_b$  at each step of doping and keeping the original geometry of  $TiB_n$ . The binding energies  $E_b$  are listed in Table 2. As can be seen in Fig. 3, we have recorded the  $E_b$  of this  $TiB_nN_{10-n}$  system as a function of the number of nitrogen atoms  $n$  for ( $n = 10$  to 0). For  $n = 10$  we still have the system  $TiB_{10}$ . For  $n = 9$  means the first doping occurs by replacing the first nitrogen with boron atom to get  $TiB_9N_1$  with an  $E_b$  of 4.19 eV/atom. The next value  $n = 8$  means  $TiB_8N_2$  and the corresponding binding energy is about 4.42 eV/atom. The  $E_b$  values increase with increasing the number of nitrogen atoms until arriving the maximum of this function labelled by  $n = 5$  achieving an  $E_b$  of 5.01 eV/atom. Afterwards the  $E_b$  function of  $TiB_nN_{10-n}$  decreases down to 2.70 eV/atom with increasing the number of nitrogen atoms until  $TiN_{10}$ . The substitution of nitrogen atoms occurs first alternately, like b–n–b–n, until  $n = 5$  obtaining symmetrical wheel  $TiB_5N_5$ , afterwards the residual boron atoms will be replaced by nitrogen one by one. The  $E_b$  function of the  $TiB_nN_{10-n}$  system is assigned by red squares.

### 3.4. The $TiC_nN_{10-n}$ system

We proceed in the same manner doping now the  $TiN_{10}$  system with carbon atoms. Starting by  $n = 1$  and replacing one nitrogen by a carbon atom we receive the molecular wheel  $TiC_1N_9$  with an  $E_b$  of 2.91 eV/atom. The next step is assigned by substituting the next nitrogen atom by carbon getting for  $n = 2$  the wheel  $TiC_2N_8$ . The

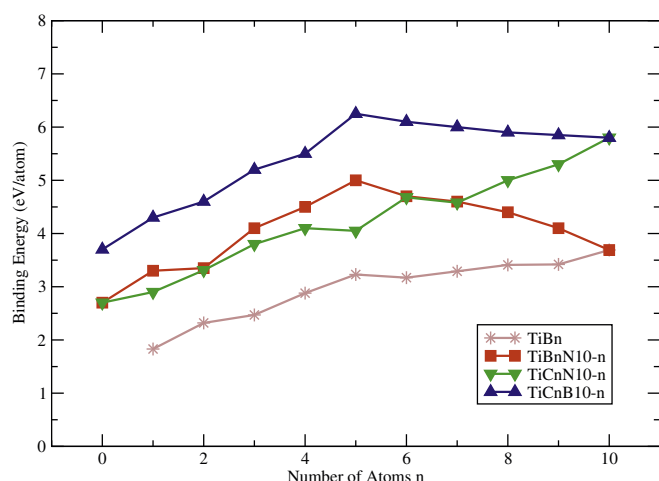


Fig. 3. Stability of clusters and molecular wheels.

Table 1

Dimension, Structure, Symmetry(State),  $E_b$  binding energy, determined at the HF-SCF/STO-3G level of theory.

Dimension	Structure	Symmetry(State)	$E_b$ (eV/atom)
2D Clusters	TiB-Linear	$C_{\infty v}(^2\Sigma_g)$	1.83
	TiB <sub>2</sub> -Planar	$C_{2v}(^3B_2)$	2.32
	TiB <sub>3</sub> -Planar	$C_{2v}(^2B_2)$	2.47
	TiB <sub>4</sub> -Planar	$C_{2v}(^3B_2)$	2.88
	TiB <sub>5</sub> -Planar	$C_{2v}(^2B_2)$	3.23
	TiB <sub>6</sub> -Planar	$C_{2v}(^3A_1)$	3.17
	TiB <sub>7</sub> -Planar	$C_{2v}(^2A_1)$	3.29
	TiB <sub>8</sub> -Planar	$C_{2v}(^3B_2)$	3.41
	TiB <sub>9</sub> -Planar	$C_{2v}(^2B_2)$	3.42
	TiB <sub>10</sub> -Wheel	$D_{2h}(^3B_{3g})$	3.69
3D Clusters	TiB <sub>3</sub> -Trigonal Pyramid	$C_{3v}(^4A_1)$	2.05
	TiB <sub>4</sub> -Tetragonal Pyramid	$C_{4v}(^3A_1)$	2.42
	TiB <sub>5</sub> -Pentagonal Pyramid	$C_{5v}(^+A')$	3.07
	TiB <sub>6</sub> -Hexagonal Pyramid	$C_{6v}(^3A_1)$	3.11
	TiB <sub>7</sub> -Heptagonal Pyramid	$C_{7v}(^2A_1)$	3.25
	TiB <sub>8</sub> -Octagonal Pyramid	$C_{8v}(^3B_1)$	3.30
	TiB <sub>9</sub> -Octagonal Umbrella	$C_{2v}(^2B_2)$	3.37
	TiB <sub>10</sub> -Nonagonal Umbrella	$C_s(^3A'')$	3.56

corresponding  $E_b$  is about 3.31 eV/atom. However, The calculated  $E_b$  values of this system are also listed in Table 2. Further steps are continued by replacing nitrogen by carbon atoms one by one in clockwise direction obtaining for  $n = 10$  the cluster  $TiC_{10}$  with an  $E_b$  of 5.80 eV/atom. The substitution of nitrogen by carbon atoms occurs first alternately, like c–n–c–n, until  $n = 5$  obtaining the symmetrical wheel  $TiC_5N_5$ . Afterwards for  $n \geq 6$  the residual nitrogen atoms are replaced by carbon one by one. It is to observe that the  $E_b$  function of the  $TiC_nN_{10-n}$  system, as shown in Fig. 3 and assigned by a green triangle down, increases upwards with increasing the number of carbon atoms  $n$ .

### 3.5. The $TiC_nB_{10-n}$ system

The substitution of carbon with boron atoms up to  $n = 5$  occurs first alternately receiving the wheel system  $TiC_5B_5$ , with the corresponding  $E_b$  listed in Table 2. Afterwards the residual carbon atoms will be replaced by boron atoms approaching the  $TiB_{10}$  system once again. As can be seen in Fig. 3, the  $E_b$  function increases with increasing the number of boron atoms up to  $n = 5$ . Thereafter it drops towards the  $E_b$  value of 3.69 eV/atom of the wheel  $TiB_{10}$ . A distinguishable maximum in Fig. 3 can be observed by  $n = 5$  corresponding to the largest  $E_b$  value of 6.25 eV/atom for the symmetrical molecular wheel  $TiC_5B_5$ . The next stable wheel is the  $TiC_6B_4$  with an  $E_b$  of 6.10 eV/atom, calculated at the HF-SCF/STO-3G

Table 2

The  $E_b$ /atom (eV) of  $TiB_nN_{10-n}$ ,  $TiC_nB_{10-n}$  ( $n = 10$  to 0) &  $TiC_nN_{10-n}$  ( $n = 0-10$ ) molecular wheels, calculated at the HF-SCF/STO-3G level.

$TiB_nN_{10-n}$	$E_b$	$TiC_nN_{10-n}$	$E_b$	$TiC_nB_{10-n}$	$E_b$
$TiB_{10}N_0^a$	3.69	$TiC_0N_{10}^b$	2.70	$TiC_{10}B_0^c$	5.80
$TiB_9N_1$	4.19	$TiC_1N_9$	2.91	$TiC_9B_1$	5.85
$TiB_8N_2$	4.42	$TiC_2N_8$	3.31	$TiC_8B_2$	5.91
$TiB_7N_3$	4.61	$TiC_3N_7$	3.82	$TiC_7B_3$	6.01
$TiB_6N_4$	4.79	$TiC_4N_6$	4.10	$TiC_6B_4$	6.10
$TiB_5N_5$	5.01	$TiC_5N_5$	4.05	$TiC_5B_5$	6.25
$TiB_4N_6$	4.52	$TiC_6N_4$	4.68	$TiC_4B_6$	5.50
$TiB_3N_7$	4.11	$TiC_7N_3$	4.58	$TiC_3B_7$	5.20
$TiB_2N_8$	3.35	$TiC_8N_2$	5.01	$TiC_2B_8$	4.62
$TiB_1N_9$	3.30	$TiC_9N_1$	5.30	$TiC_1B_9$	4.33
$TiB_0N_{10}^b$	2.70	$TiC_{10}N_0^c$	5.80	$TiC_0B_{10}^a$	3.69

<sup>a</sup>  $TiB_{10}N_0$  and  $TiC_0B_{10}$  means  $TiB_{10}$ .

<sup>b</sup>  $TiB_0N_{10}$  and  $TiC_{10}N_0$  means  $TiN_{10}$ .

<sup>c</sup>  $TiC_{10}N_0$  and  $TiC_0B_{10}$  means  $TiC_{10}$ .

level of theory, as the case of whole substitutions in the  $\text{TiC}_n\text{B}_{10-n}$  system. Both molecular wheels  $\text{TiC}_5\text{B}_5$  and  $\text{TiC}_6\text{B}_4$  are represented in Fig. 4. The distribution of the  $E_b$  function of the  $\text{TiC}_n\text{B}_{10-n}$  system is assigned in Fig. 3 by a blue triangle up. However, further computations beyond the HF-SCF level show that the sequence of the stability of both wheels  $\text{TiC}_5\text{B}_5$  and  $\text{TiC}_6\text{B}_4$  is reversed when considering the functionals B3LYP and 6-31G basis set [17].

### 3.6. The $\text{MeC}_5\text{B}_5$ system

In order to understand the nature of chemical bonds of metal atoms with boron and carbon wheels we have computed the wheel system  $\text{MeC}_5\text{B}_5$  considering for Me the first row of transition metal atoms  $\text{Me} = \text{Sc}, \text{Ti}, \text{V}, \text{Cr}, \text{Mn}, \text{Fe}, \text{Co}, \text{Ni}, \text{Cu},$  and  $\text{Zn}$ . Of course higher spin multiplicity could mean lower ground state energy of individual metal atoms. However, we have optimized each structure at the HF-SCF/6-31G level of theory, and calculated the ground state energies at different spin states for each metal atom. We selected the lowest energy and determined the corresponding binding

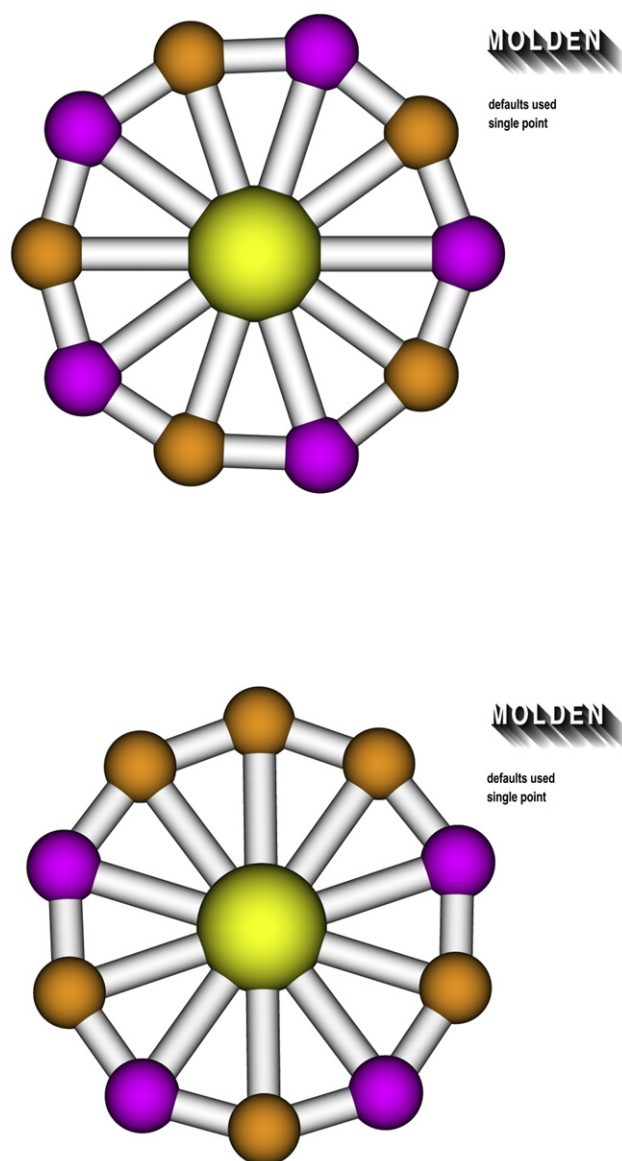


Fig. 4. Molecular wheels of  $\text{TiC}_5\text{B}_5$  and  $\text{TiC}_6\text{B}_4$ .

Table 3

The molecular wheels  $\text{MeC}_5\text{B}_5$ , where Me is the first row of transition metal atoms calculated at the HF-SCF/6-31G level of theory, symmetry and spin state, binding energy  $E_b$ /atom (eV), and bondlength  $R$  (Å).

$\text{MeC}_5\text{B}_5$	Sym./State	$E_b$	$R_{\text{MeC}}$	$R_{\text{MeB}}$	$R_{\text{BC}}$
$\text{ScC}_5\text{B}_5$	$D_{5h}({}^3A_1')$	3.75	2.34	2.31	1.44
$\text{TiC}_5\text{B}_5$	$D_{5h}({}^4A_1')$	3.70	2.28	2.33	1.43
${}^a\text{VC}_5\text{B}_5$	$C_{2v}({}^3B_1)$	3.22	2.26	2.32	1.41
${}^a\text{CrC}_5\text{B}_5$	$C_{2v}({}^2B_1)$	3.15	2.26	3.34	1.42
$\text{MnC}_5\text{B}_5$	$D_{5h}({}^1A_1')$	3.80	2.24	2.30	1.41
$\text{FeC}_5\text{B}_5$	$D_{5h}({}^8A_1')$	3.70	2.34	2.29	1.43
${}^a\text{CoC}_5\text{B}_5$	$C_{2v}({}^3A_2)$	3.10	2.28	2.31	1.42
$\text{NiC}_5\text{B}_5$	$D_{5h}({}^8A_1')$	3.11	2.44	2.27	1.46
$\text{CuC}_5\text{B}_5$	$D_{5h}({}^1A_1')$	3.01	2.41	2.21	1.44
${}^a\text{ZnC}_5\text{B}_5$	$C_{2v}({}^4A_2)$	3.35	2.36	2.29	1.44

<sup>a</sup> These wheels have  $D_{5h}$  symmetry but calculated in  $C_{2v}$  one.

Molecular Wheels (Me C\_5 B\_5)

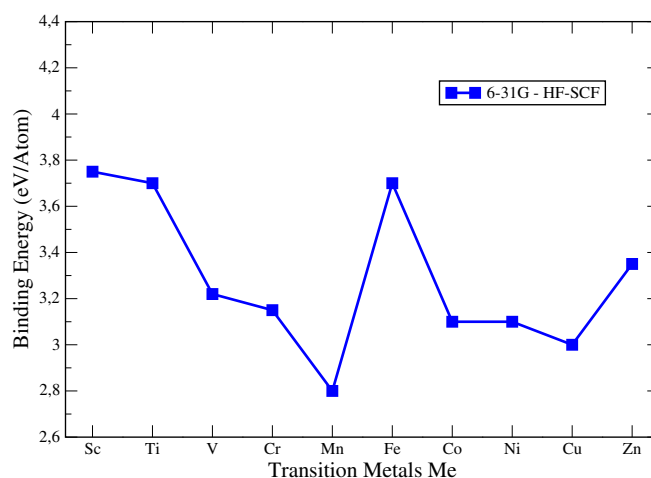


Fig. 5. Stability of molecular wheel  $\text{MeC}_5\text{B}_5$ .

energy, symmetry, spin state and bondlengths between the central and peripheral atoms as well as between carbon and boron atoms, all are listed in Table 3. The calculated  $E_b$ , as defined in eq (1), is plotted in Fig. 5 as a function of the metal atoms. As shown in Fig. 5, the molecular wheel  $\text{MeC}_5\text{B}_5$  favours Sc atom at the centre, but also Ti or Fe are the next favoured transition metal atoms. The spin multiplicity considered in the  $\text{MeC}_5\text{B}_5$  wheels for the Sc, Ti and Fe atoms was triplet, quadruplet and octuplet, respectively. In Fig. 5, the  $E_b$  function of the system  $\text{MeC}_5\text{B}_5$ , determined at the HF-SCF/6-31G level, is represented by blue squares. However, further computations of  $\text{MeC}_5\text{B}_5$  and  $\text{MeC}_6\text{B}_4$  in a follow-up study [17] are running at higher level of theory to verify the final stability of these structures.

## 4. Summary and conclusions

Based on the fact that small boron clusters  $\text{B}_n$  ( $n \leq 19$ ) have planar or quasiplanar structures, we have doped boron clusters with transition metal atoms and enquired whether the planarity would keep consistent. Therefore we have investigated 2D and 3D structures of  $\text{TiB}_n$  for ( $n \leq 10$ ) using simple STO-3G basis set at the HF-SCF level of theory. The 2D  $\text{TiB}_n$  structures where chosen to be flat where Ti is at the focus and the boron atoms located at one side forming arcs and growing up to cycles or precisely to molecular wheels. The 3D structures of  $\text{TiB}_n$  where chosen to be pyramids

where Ti is always as an apex atom. The obtained structure of the wheel of  $\text{TiB}_{10}$  was fixed, then boron atoms were replaced by nitrogen then by carbon one by one. The metal atom in the most stable molecular wheel of  $\text{TiB}_5\text{C}_5$  was then replaced by all atoms of the first row of transition metals.

We have developed 2D  $\text{TiB}_n$  system starting by two atomic molecule  $\text{TiB}$  adding boron atoms as long as the cycle closes gaining a wheel. Because of similarity, we present in Fig. 1 selected 2D  $\text{TiB}_n$  clusters for  $n = 3, 4, 6, 8$  and 10. We have also determined 3D clusters of  $\text{TiB}_n$  in form of pyramids to show that the 3D pyramidal structures are energetically less favoured. Due to similarity, we present in Fig. 2 selected 3D  $\text{TiB}_n$  clusters for  $n = 3, 4, 6, 8$  and 10. The  $E_b$  of 2D and 3D structures are listed in Table 1. The  $E_b$  of the 2D  $\text{TiB}_n$  system is presented in Fig. 3 as a function of cluster size. As can be seen, it increases with increasing the number of boron atoms  $n$  arriving the maximal value 3.69 eV/atom for  $n = 10$ . Furthermore, we have doped the  $\text{TiB}_n$  system with nitrogen atoms by substituting boron first alternately then completely with nitrogen atoms receiving the  $\text{TiB}_n\text{N}_{10-n}$  system. For  $n = 10$  we have the original system  $\text{TiB}_n$ , but for  $n = 9$  we dope the first nitrogen atom obtaining  $\text{TiB}_9\text{N}_1$  and improving its stability. Further doping with nitrogen atoms improves the stability upwards until fivefold substitutions of boron with nitrogen atoms alternately we reach with 5.0 eV/atom the maximum of the  $E_b$  of the  $\text{TiB}_5\text{N}_5$  wheel. Replacing the residual boron atoms by nitrogen up to  $\text{TiN}_{10}$  the stability diminishes down to a value of 2.7 eV/atom.

We follow the same procedure in the  $\text{TiB}_n\text{N}_{10-n}$  system by keeping the nitrogen atoms and substituting boron by carbon atoms to produce the  $\text{TiC}_n\text{N}_{10-n}$  system. We embrace the issue whether carbon can rebuild and re-establish the lost stability. The substitution of nitrogen by carbon atoms follows first alternately then completely causing progression in stability up to an  $E_b$  value of 5.8 eV/atom for the  $\text{TiC}_{10}$  wheel. However, further substitution of carbon with boron into the system  $\text{TiC}_n\text{B}_{10-n}$  leads to increment the stability achieving by  $n = 5$  another maximum of stability of 6.26 eV/atom, obtaining the wheel  $\text{TiC}_5\text{B}_5$ . Afterwards the stability decreases so far until the carbon atoms are completely replaced by boron returning back to the wheel  $\text{TiB}_{10}$ , obtained by the first route, with the original  $E_b$  value 3.69 eV/atom. After structural optimization of  $\text{TiC}_5\text{B}_5$ , we found that the distance between Ti and carbon atoms is shorter as to boron atoms. Thus, the atomic distance between the centre Ti and peripheral atoms B and C is respectively 2.27 and 2.21 Å, while the bondlength of B–C is about 1.38 Å. As mentioned above, we will see in the follow-up paper [17] that at the B3LYP functionals and 6-31G basis set the  $\text{TiC}_6\text{B}_4$  wheel is with 0.04 eV/atom slightly more stable than the  $\text{TiC}_5\text{B}_5$ .

All systems studied above where carried out considering the transition metal atom Ti. Now arises the question: could another atom of the first row of transition metals induce better stability!. Therefore we have established further computations at the HF-SCF/6-31G level to determine the  $\text{MeC}_5\text{B}_5$  system for  $\text{Me} = \text{Sc}$  to  $\text{Zn}$ . These calculations are presented in Fig. 5 showing that Sc atom at the centre exhibits the highest binding energy, followed by Ti then by Fe atoms. In the second part of this work [17] we will ascertain that the wheel  $\text{TiC}_6\text{B}_4$  at the B3LYP/6-31G level is energetically favoured over the  $\text{ScC}_5\text{B}_5$  one.

We conclude that we have developed a new path of molecular wheels and determined how to increase the stability of molecular structures by substituting boron by nitrogen and carbon. However, the behaviour of the binding energy in increasing and dropping seems to depend on the ratio and sequence of the involved boron, nitrogen and carbon atoms around the central titanium atom. Consequently, a further study at higher quality basis sets and functionals is in progress [17] to verify these points mentioned above. We have established that metal boride clusters favour 2D

structures forming molecular wheels similar to those cyclic rings of the boron wheel  $\text{B}_8$  [3], to carbon rings [9] or to boron carbide wheels [11]. In addition, the  $\alpha$ -, and  $\beta$ -spin HOMO–LUMO gaps of  $\text{TiB}_{10}$  are 0.330 and 0.253 Hartree, respectively. Slightly larger HOMO–LUMO gaps of  $\alpha$ - and  $\beta$ -spin were found for the  $\text{TiC}_5\text{B}_5$  wheel to be 0.363 and 0.263 Hartree, respectively. These HOMO–LUMO gaps values 0.90 and 0.27 eV of  $\alpha$ - and  $\beta$ -spin of  $\text{TiC}_5\text{B}_5$  versus those of  $\text{TiB}_{10}$  are a clear evidence for the stabilization character of carbon atoms involved into the wheel.

According to the Mulliken analysis, the electron charge transfer in the most stable molecular wheel  $\text{TiC}_5\text{B}_5$  at the HF-SCF/STO-3G level of theory occurs slightly from titanium and boron to carbon atoms. The extent of electron charge of titanium and the average of five boron atoms is respectively 0.854 and 0.136 e, while the average of the charge transfer to the five carbon atoms is likely  $-0.306$  e. In contrast, the electron transfer in  $\text{TiB}_{10}$  occurs with 0.450 e from the Ti atom to the each of the ten boron atoms to achieve a charge of  $-0.045$  e, approving the true electron deficient character of boron. The variation of the stability of the molecular wheels over the transition metal as central atoms, as represented in Fig. 5, gives no insight about the reason. However, in our follow-up study we will try to verify the role and number of d-electrons and their contributions in bonding and character as well as the correlation between the p- and d-electrons. Calculations on molecular wheel systems  $\text{MeB}_x\text{C}_y\text{N}_z$ , for different combinations of nonzero  $x$ ,  $y$  and  $z$ , are still missing. Also some electronic properties like vibrational frequencies, bond order analysis, and aromaticity in connection with the  $\pi$ -orbitals are desirable.

## References

- [1] R.N. Grimes, J. Chem. Educ. 81 (2004) 657.
- [2] V. Bonačić-Kouteck, P. Fantucci, J. Kouteck, Chem. Rev. 91 (1991) 1053.
- [3] I. Boustani, Phys. Rev. B 55 (1997) 16426.
- [4] H.J. Zhai, B. Kiran, J.L. Li, L.S. Wang, Nat. Mater. 2 (2003) 827.
- [5] W. Huang, A.P. Sergeeva, H.-J. Zhai, B.B. Averkiev, L.-S. Wang, A.L. Boldyrev, Nat. Chem. 2 (2010) 202.
- [6] I. Boustani, Z. Zhu, D. Tomanek, Phys. Rev. B 83 (2011) 193405.
- [7] M. Menon, K.R. Subbaswamy, M. Sawtarie, Phys. Rev. B 48 (1993) 8398.
- [8] Z. Slanina, S.-L. Lee, M. Smigel, J. Kurtz, L. Adamowicz, Mat. Res. Symp. Proc. 359 (1995) 163.
- [9] R.O. Jones, G. Seifert, Phys. Rev. Lett. 79 (1997) 443.
- [10] H. Werheit, A. Leithe-Jasper, T. Tanaka, H.W. Rotter, K.A. Schwetz, J. Solid State Chem. 177 (2004) 575.
- [11] S.S. Park, Bull. Korean Chem. Soc. 26 (2005) 63.
- [12] W. Sekkal, B. Bouhafs, H. Aourag, M. Certier, J. Phys. Condens. Matter 10 (1998) 4975.
- [13] X.-B. Wang, C.-F. Ding, L.-S. Wang, J. Phys. Chem. A 101 (1997) 7699.
- [14] X. Liu, G.-F. Zhao, L.-J. Guo, Q. Jing, Y.-H. Luo, Phys. Rev. A 75 (2007) 063201.
- [15] Z. Pu, K. Ito, P. v. R. Schleyer, Q.-S. Li, Inorg. Chem. 48 (2009) 10679.
- [16] I.-W. Park, K.H. Kim, A.O. Kunnath, D. Zhong, J.J. Moore, A.A. Voevodin, E.A. Levashov, J. Vac. Sci. Technol. B 23 (2005) 588.
- [17] A. Güthler, M. B. D. Andaloussi, R. Pandey, I. Boustani, in preparation.
- [18] Gaussian 03, Revision C.02, M. J. Frisch, G. W. Trucks, H. B. Schlegel, G. E. Scuseria, M. A. Robb, J. R. Cheeseman, J. A. Montgomery, Jr., T. Vreven, K. N. Kudin, J. C. Burant, J. M. Millam, S. S. Iyengar, J. Tomasi, V. Barone, B. Mennucci, M. Cossi, G. Scalmani, N. Rega, G. A. Petersson, H. Nakatsuji, M. Hada, M. Ehara, K. Toyota, R. Fukuda, J. Hasegawa, M. Ishida, T. Nakajima, Y. Honda, O. Kitao, H. Nakai, M. Klene, X. Li, J. E. Knox, H. P. Hratchian, J. B. Cross, C. Adamo, J. Jaramillo, R. Gomperts, R. E. Stratmann, O. Yazyev, A. J. Austin, R. Cammi, C. Pomelli, J. W. Ochterski, P. Y. Ayala, K. Morokuma, G. A. Voth, P. Salvador, J. J. Dannenberg, V. G. Zakrzewski, S. Dapprich, A. D. Daniels, M. C. Strain, O. Farkas, D. K. Malick, A. D. Rabuck, K. Raghavachari, J. B. Foresman, J. V. Ortiz, Q. Cui, A. G. Baboul, S. Clifford, J. Cioslowski, B. B. Stefanov, G. Liu, A. Liashenko, P. Piskorz, I. Komaromi, R. L. Martin, D. J. Fox, T. Keith, M. A. Al-Laham, C. Y. Peng, A. Nanayakkara, M. Challacombe, P. M. W. Gill, B. Johnson, W. Chen, M. W. Wong, C. Gonzalez, J. A. Pople, Gaussian, Inc., Wallingford CT, 2004.
- [19] GAMESS-UK is a package of ab initio programs. See: <http://www.cfs.dl.ac.uk/game-uk/index.shtml> M.F. Guest, I.J. Bush, H.J.J. van Dam, P. Sherwood, J.M.H. Thomas, J.H. van Lenthe, R.W.A. Havenith, J. Kendrick, The GAMESS-UK electronic structure package: algorithms, developments and applications, Mol. Phys. 103 (2005) 719–747.
- [20] T.B. Tai, D.J. Grant, M.T. Nguyen, D.A. Dixon, J. Phys. Chem. A 114 (2010) 944.
- [21] A.N. Alexandrova, A.L. Boldyrev, H.-J. Zhai, L.S. Wang, Coord. Chem. Rev. 250 2811 (2006).